Specific inhibition of TRPV4 enhances retinal ganglion cell survival in adult porcine retinal explants

Taylor, Linnéa; Arnér, Karin; Ghosh, Fredrik

Published in:
Experimental Eye Research

DOI:
10.1016/j.exer.2016.11.002

2017

Document Version:
Peer reviewed version (aka post-print)

SPECIFIC INHIBITION OF TRPV4 ENHANCES RETINAL GANGLION CELL SURVIVAL IN ADULT PORCINE RETINAL EXPLANTS

Linnéa Taylor, Karin Arnér, Fredrik Ghosh

Department of Ophthalmology, Lund University, SE 22184, Lund, Sweden

Corresponding author:

Linnéa Taylor

Department of Ophthalmology

Lund University

S-22184 Lund, Sweden

phone:+46 46 2220770

fax: +46 46 2220774

e-mail: linnea.taylor@med.lu.se

ABSTRACT

Signaling through the polymodal cation channel Transient Receptor Potential Vanilloid 4 (TRPV4) has been implicated in retinal neuronal degeneration. To further outline the involvement of this channel in this process, we here explore modulation of Transient Receptor Potential Vanilloid 4 (TRPV4) activity on neuronal health and glial activation in an in vitro model of retinal degeneration. For this purpose, adult porcine retinal explants were cultured using a previously established standard protocol for up to 5 days with specific TRPV4 agonist GSK1016790A (GSK), or specific antagonist RN-1734, or culture medium only. Glial and neuronal cell health were evaluated by a battery of immunohistochemical markers, as well as morphological staining. Specific inhibition of TRPV4 by RN-1734 significantly enhanced ganglion cell survival, improved the maintenance of the retinal laminar architecture, reduced apoptotic cell death and attenuated the gliotic response as well as preserved the expression of TRPV4 in the plexiform layers and ganglion cells. In contrast, culture controls, as well as specimens treated with GSK, displayed rapid remodeling and neurodegeneration as well as a downregulation of TRPV4 and the Müller cell homeostatic mediator glutamine synthetase. Our results indicate that TRPV4 signaling is an important contributor to the retinal degeneration in this model, affecting neuronal cell health and glial homeostasis. The finding that pharmacological inhibition of the receptor significantly **attenuates neuronal degeneration and gliosis in vitro**, suggests that TRPV4 signaling may be an interesting pharmaceutical target to explore for treatment of retinal degenerative disease.

Keywords: retina, TRPV4, ganglion cells, gliosis, retinal degeneration

1. INTRODUCTION

The polymodal cation channel Transient Receptor Potential Vanilloid 4 (TRPV4) has a wide range of cellular functions, including osmosensation and mechanosensation [1-4]. The channel can be activated by a a variety of stimuli involved in cell and tissue stress, including membrane stretch, elevated pressure, heat, polyunsaturated fatty acids, endocannabinoids and cytochrome P450-derived metabolites [1-4]. Activation of the channel results in Ca2+ influx, which by nature is very rapid [5].

In the brain, TRPV4 is widely expressed in neurons and glia [2,3]. Recently, TRPV4 signaling has been implicated in a numerous neurodegenerative disorders. For instance, gain-of-function mutations in the TRPV4 gene, resulting in Ca2+ overload and neuronal degeneration, has been suggested to be the mechanism behind type II hereditary motor and sensory neuropathies [6]. Increased TRPV4 expression and activation has been found to coincide with gliosis after cerebral hypoxia/ischemia, and glial-expressed TRPV4 has been reported to mediate infrasound-induced neuronal degeneration in vibroacoustic disease [2,4, 7].

Recently, it has been found that the retina also contains TRPV4, mainly on Müller glia, retinal ganglion cells (RGCs) and at the optic nerve head [3]. Here, sustained activation of TRPV4 has been shown to lead to apoptosis in RGCs, as well as Müller cell gliosis, suggesting a possible role during retinal degenerative pathologies such as glaucoma [3,8].

Rapid RGC death is a well-described feature of an established in vitro model of retinal degeneration involving cultured adult full-thickness retinal sheets [9-14]. Adult porcine retinal explants cultured with the photoreceptors apposed against the culture membrane begin to display neuronal degeneration within 24h, with significant RGC loss already after 3h [10, 12-16]. The degeneration of RGCs in this model can be attenuated

by providing the inner retina with mehanical support, although the mechanism behind this phenomenon remains to be elucidated [14]. The use of adult porcine retina is useful in this setting, as it closely resembles the human counterpart in terms of size, retina vasculature and rod-and-cone distribution.

For this paper, our hypothesis was that TRPV4 signaling may be involved in the rapid demise of RGCs in this model, and that inhibition of TRPV4 activity would result in RGC rescue. We herein describe the effects of modulating TRPV4 signaling through specific TRPV4 agonist GSK1016790A and specific TRPV4 antagonist RN-1734 on neurons and glial cells in adult porcine retinal explants.

2. MATERIAL AND METHODS

2.1 Tissue Culturing

All proceedings and animal treatment were in accordance with the guidelines and requirements of the government committee on animal experimentation at Lund University and with the ARVO statement on the use of animals in ophthalmic and vision research. The study was approved by the Malmö-Lund committee on Animal Research Ethics. Eyes were harvested from adult female pigs aged between 4-6 months euthanized by an overdose of sodium pentobarbital (Apoteket, Umeå, Sweden). The neuroretinas were removed using a previously described method [12]. To summarize, the eyes were enucleated immediately after euthanization and placed in ice-cold CO_2 –independent medium (Invitrogen, Paisley, UK). A sharp incision was made in the pars plana, removing the anterior segment by cutting 360 degrees. The neuroretinas were gently removed from the pigment epithelium using microforceps, and cutting at the optic nerve head using microscissors. Each neuroretina was sectioned into 6 pieces, measuring approximately 8x8 mm. In total, 23 eyes from 12 animals were used, yielding 98 specimens for culture and 6 eyes serving as a normal adult in vivo controls. The 98 neuroretinal pieces were explanted onto Millicell- PCF 0.4 μm culture plate inserts (Millipore, Billerica, MA, USA), with the photoreceptors facing the membrane. **Specimens were divided into four groups, and cultured in either baseline medium (DMEM/F12 (Invitrogen), containing 1.05mM $CaCl_2$, with 10% fetal calf serum added (Sigma-Aldrich, St Louis, MO, USA;controls; CT), or using baseline medium with the following supplementation: RN-1734, a specific TRPV4 antagonist (RN; 5μM; (Millipore, Billerica, MA, USA), or GSK1016790A, a highly potent and specific TRPV4 agonist (GSK; 10nM; Sigma-Aldrich, St Louis, MO, USA) and maintained at 37 °C at 95% humidity and 5% CO2. Supplementation concentrations were based on previously**

reported in vitro experiments [3, 17-19]. RN-1734 has been observed to completely inhibit both ligand- and hypotonicity-activated TRPV4, as well as being selective for TRPV4 in a TRP selectivity panel including TRPV1, TRPV3 and TRPM8 [33]. GSK1016790A has been shown to be a more specific and potent activator compared to the traditionally used phobol ester 4α-PDD, and has been found to activate TRPV4 in a range of cell types [17]. Explants originating from the same animal were divided among the various culture groups to ensure no bias. The medium was exchanged every second day. Explants were fixed at 1, 2 and 5 DIV.

2.2 Histology

Histological examinations were performed as previously described [12], and only briefly summarized here. After culturing, the explants were fixed in 4% paraformaldehyde in 0.1M phosphate buffer, pH 7.2 for 2h in 4 °C. The normal adult in vivo controls were fixed immediately after harvest using the same paraformaldehyde concentration for 8h in 4°C. The explants were then infiltrated with 0.1M Sörensens medium with increasing concentrations of sucrose up to 25% for cryoprotection. The fixed, cryoprotected explants were embedded in egg albumin/gelatine medium for cryosectioning at -20 °C, with a section thickness of 12 µm. For morphological analysis, every 10th slide was stained with hematoxylin and eosin. For immunohistochemical labeling, adjoining slides with sections originating from the center of the explants were chosen. The specimens were rinsed 3 times with PBS containing 0.1% Triton- X, and then incubated with PBS containing 0.1% Triton-X and 1% bovine serum albumin (BSA) for 20 minutes at room temperature. After this, the specimens were incubated overnight at 4 °C with the respective primary antibody (Table 1). In the double labeling for TRPV4 and NeuN, both primary antibodies were added at this stage. The specimens were

then rinsed in PBS-Triton-X (0.1%), and incubated for 45 minutes with a secondary fluorescein isothiocyanate (FITC) and/or Rhodamine Red-conjugated antibody (Table 1), and then mounted in Vectashield mounting medium (Vector laboratories Inc., CA, USA). Negative control experiments were performed as above, replacing the primary antibody with PBS containing 0,1% Triton-X and 1% BSA. Normal adult pig retina was used as a positive control.

Terminal deoxynucleotidyl transferase dUTP nick end labeling (TUNEL) staining was performed according to the manufacturer's instructions, using a TMR red In Situ Cell Death Detection kit (Roche Diagnostics GmbH, Mannheim, Germany).

2.2.1 Microscopy, image analysis and statistical analysis

The histological sections and immunohistochemically labeled specimens were examined using an optical and epifluorescence microscope (Axio Imager M2, Carl Zeiss Microscopy GmbH, Jena, Germany) equipped with a digital camera system (AxioCam MRm, Carl Zeiss Microscopy GmbH) and a digital acquisition system (ZEN 2012 blue edition, Carl Zeiss Microscopy GmbH). When comparing immunolabeled sections, all specimens were processed in one batch for each labeling, and were photographed blindly in one session using a fixed exposure time and aperture. To generate temporal profile of changes in NeuN-labeled cells, Recoverin-labeled cell rows, TUNEL labeling intensity as well as glial fibrillary acidic protein (GFAP) and glutamine synthetase (GS) and TRPV4 protein expression, 2-3 images of 3-4 sections originating from the central portion of all specimens were taken. ImageJ was used to obtain labeling intensity measurements (Rasband, W.S., ImageJ, U. S. National Institutes of Health, Bethesda, Maryland, USA, http://imagej.nih.gov/ij/, 1997-2014), with a protocol described previously[20]. The photographs were obtained in batches, as detailed above. All samples were photographed using a fixed exposure time and 20x magnification.

For cell counts, values are given as labeled cells/450 microns or cell rows/450 microns. In the pig, the NeuN antibody strongly labels ganglion cells in the ganglion cell layer, and weakly labels displaced amacrine cells in the inner nuclear layer and inner plexiform layer [12,13]. For analysis of ganglion cells, only large, strongly labeled cells of a ganglion morphology located in the ganglion cell layer were counted. For GFAP labeling intensity measurements, a rectangular area of 770x545 pixels was analyzed, placed so it spanned the specimen from below the astrocytic layer/endfeet at the inner border, to the outer border of the ONL, ensuring no interference from autofluorescence in the inner and outer segments or native GFAP expression in the astrocytes and endfeet. For GS and total TUNEL labeling, the area of interest was placed so it spanned the retina from inner to outer border, excluding the inner and outer segments. For TUNEL layer measurements, an area was selected spanning the width of the specimens, including only the cellular layer of interest. The background was subtracted and the mean fluorescence measurement was recorded. All cell counts and fluorescence intensity measurements were performed blindly. The data was analyzed using a one-way ANOVA with a Tukey post hoc test (GraphPad InStat; GraphPad Software, San Diego, CA, USA). Raw data from intensity measurements and cell counts were used to generate mean values for each of the different groups. Values of $p<0.05$ were considered significant. A representative image for the figure panels was chosen from each batch.

3. RESULTS

3.1 In vivo controls

As predicted, hematoxylin and eosin staining (HTX) of normal adult porcine retina in vivo showed clear lamination and well-populated cell layers (Fig. 1A). Sections labeled with NeuN displayed labeling of large cell bodies of ganglion morphology located in the ganglion cell layer (GCL), as well as scattered, very weakly labeled displaced amacrine cells located in the inner plexiform layer (IPL; Fig. 1B). Recoverin labeling of rod and cone photoreceptors showed strong labeling of cell bodies in the outer nuclear layer (ONL) as well as inner and outer segments (Fig. 1C). Glial fibrillary acidic protein (GFAP) labeling revealed strong labeling of Müller cell endfeet and astrocytes at the inner border, as well as weaker labeling of vertical fibers spanning the inner layers (Fig. 1D). Strong, diffuse labeling of Glutamine Synthetase (GS) was present mainly in the innermost parts of Müller cells, with weak labeling of vertical processes spanning the IPL and inner nuclear layer (INL), which is normal for this species (Fig 1E) [12]. TRPV4 labeling was present in ganglion cells, in both plexiform layers, and at the inner border in structures corresponding to Müller cell endfeet (Fig. 1F). A double-labeling of TRPV4 and NeuN revealed punctate labeling of TRPV4 in NeuN-positive cells (Fig. 1G). No TUNEL labeled cells were observed (Fig 1H).

3.2 Cultured explants

HTX staining of control explants (CT) and explants treated with the TRPV4 agonist GSK1016790A (GSK) kept for 1 DIV revealed numerous pyknotic cells in all nuclear layers. These layers appeared slightly disorganized with large vacuoles were present in the INL (Fig. 2A-B). In contrast, explands the TRPV4 specific antagonist RN-1734 (RN) revealed a well populated GCL with numerous large cells of ganglion morphology, only scattered pyknotic

cells in the nuclear layers, and inner segments lining the outer border of the ONL (Fig 2C). 2 DIV CT explants appeared thin, with pyknotic cells in all cell layers (Fig. 2D). 2 DIV GSK-treated explants appeared similar to corresponding 1 DIV retinas, although the nuclear layers appeared slightly thinner and contained large vacuoles (Fig. 2E). In contrast, RN counterparts revealed thick, well populated nuclear layers, with inner segments at the outer border of the ONL, which contained scattered pyknotic cells (Fig. 2F). 5DIV CT explants, as well as GSK treated counterparts, showed thin, disorganized nuclear layers with a multitude of pyknotic cells, with large, vacuoles present throughout the inner layers (Fig. 2G-H). In contrast, corresponding RN explants displayed well-organized nuclear layers, with scattered pyknotic cells (Fig. 2I).

Recoverin labeling of rod and cone photoreceptors showed revealed a similar labeling pattern in all after 1 DIV, with labeling present in the ONL with a slightly disorganized band of inner segments and debris at the outer border, and no significant difference was found in the number of labeled cell rows (Fig. 2J-O, statistical data not shown). **After 2 DIV, CT explants showed strong labeling present in a thin ONL (Fig. 2M). In contrast, corresponding GSK specimens revealed strong labeling only in scattered cellular structures at the outer border as well as photoreceptor terminals in the inner ONL (Fig. 2N). RN counterparts displayed weak labeling of the cell bodies throughout the ONL, with strong labeling of the inner and outer borders of the ONL (Fig. 2O). No significant difference was found in the number of labeled cell rows between the various groups (statistical data not shown). After 5 DIV, CT explants revealed strong labeling of a thin, disorganized ONL (Fig. 2P). GSK treated counterparts displayed a disorganized photoreceptor layer with scattered recoverin-labeled structures at the inner and outer border of the ONL (Fig. 2Q). In contrast, RN explants displayed strong labeling of ONL**

structures as well as what appeared to be inner and outer segment debris at the outer border of the ONL (Fig. 2R). No significant difference was found in the number of labeled cell rows between the groups (statistical data not shown).

At all time points, NeuN labeling of ganglion cells revealed a significant preservation in the number of labeled cells in RN explants compared to GSK and CT counterparts (Fig. 3A-O, $p<0.001$ for all comparisons). In addition, the number of cells surviving did not vary significantly within this group from 1-5 DIV. In contrast, after 1 DIV, GSK explants displayed a dramatic reduction in the number of surviving cells, with significantly fewer cells remaining when compared to corresponding CT specimens (Fig. 3A-B, M; $p<0.01$). At 2 and 5 DIV, only isolated cells remained in CT and GSK explants (Fig. 3D-E, G-H, N-O).

GFAP labeling of explants cultured for 1 and 2 DIV showed labeling of astrocytes, as well as isolated, weakly labeled vertical processes, with no significant difference in morphology and labeling intensity between the different treatment groups (Fig. 4A-F; statistical data not shown). After 5 DIV, GSK and RN treated explants displayed a similar appearance to that observed in 1 and 2 DIV counterparts, whereas CT specimens displayed a significantly upregulated expression in hypertrophic and slightly disorganized Müller cells (Fig. 4G-J; $p<0.001$ and $p<0.01$, respectively).

GS labeling of 1 DIV retinas revealed a general downregulation of expression compared to the in vivo control (Fig. 5J). RN and GSK explants displayed a significantly higher level of GS expression compared to CT explants (Fig. 5A-C, J; $p<0.01$ and $p<0.001$, respectively). After 2 DIV, CT explants revealed labeling present in a scattered manner across the retina, with stronger labeling present at the inner border (Fig. 5D). GSK specimens showed weak labeling only at the innermost and outermost border (Fig. 5E). In contrast to GSK counterparts, RN explants displayed significantly stronger labeling, present throughout the

specimen (Fig. 5F, J; $p<0.001$). After 5 DIV, CT and GSK explants showed only weak labeling of Müller cells, whereas corresponding RN specimens displayed strong labeling present throughout the retina (Fig. 5G-I, K; $p<0.001$ and $p<0.001$ respectively).

CT1 and GSK1 explants showed only weak TRPV4 labeling present in the IPL and scattered structures at the innermost border, as well as slightly stronger labeling of the OPL (Fig. 6A-B). In contrast, RN1 specimens revealed strong labeling of the plexiform layers, at the innermost border, and in ganglion cells (Fig. 6C). 2 and 5 DIV CT and GSK retinas displayed a labeling pattern similar to that observed in 1 DIV counterparts (Fig. 6D-E, G-H). Corresponding RN explants showed strong labeling of both plexiform layers as well as ganglion cells at the inner border (Fig. 6F, I). Statistical analysis of the fluorescence intensity measurements revealed a significant preservation of TRPV4 expression in RN explants at all time points compared to CT and GSK counterparts (Fig 6J-L, $p<0.001$).

TUNEL labeling of CT1 and GSK1 explants displayed numerous apoptotic cells in all cell layers (Fig.7A-B). In contrast, RN counterparts show only weak labeling of cells mainly in the ONL, with significantly lower labeling intensity, both when comparing total labeling and layer labeling, compared to corresponding CT specimens (Fig. 7C, J; $p<0.001$; 8A, D, G). 2 DIV CT and GSK explants revealed labeling of a multitude of cells in all cell layers (Fig. 7D-E). RN counterparts revealed numerous labeled cells scattered throughout the retina, although no significant difference was observed in total labeling intensity (Fig. 7F, K; $p<0.05$). The GCL of RN explants showed significantly lower labeling intensity compared to GSK and CT counterparts (Fig 8B, E, H). After 5 DIV, all culture groups show a multitude of labeled cells, where CT explants revealed a significantly higher labeling intensity compared to GSK and RN counterparts (Fig. 7G-I,

L; p<0.05 and p<0.01, respectively). Analysis of the labeling intensity of individual cell layers showed significantly higher labeling of the INL in CT explants compared to GSK and RN counterparts (Fig. 8F, p<0.01 and p<0.001, respectively). Although the ONL and GCL also showed higher labeling intensity in CT specimens compared to corresponding GSK and RN retinas, the difference was not significant (Fig. 8C, I).

4. DISCUSSION

We and others have previously reported that full-thickness adult porcine retina cultured under standard conditions undergoes rapid neuronal degeneration and gliosis [9-12]. In the present work, we found that RN-1734 treatment in adult porcine retinal explants significantly enhances ganglion cell survival, improves maintenance of the retinal laminar architecture, reduces apoptotic cell death, and attenuates the gliotic response. This, for the first time, suggests that TRPV4 signaling is significantly involved in maintaining retinal homeostasis.

4.1 Ganglion cells

Ganglion cells have previously been reported to express TRPV4, a finding consistent with our immunohistochemical results. In CT and GSK explants, the majority of ganglion cells were lost already after 1 day in vitro. We have previously reported that this cell loss, most likely initiated by the axotomy inherent to the explantation procedure, occurs as early as 3h after explantation in this model [14]. In vivo, only approximately 50% of RGCs can be saved 3 days after axotomy, despite neurotrophic factor treatment [21]. In RN treated retinas, which displayed a preservation of approximately 65% of ganglion cells after 1 DIV, the number of surviving cells did not vary significantly over time, in contrast to CT cultures, where ganglion cell loss was progressive. GSK explants displayed significant ganglion cell degeneration already after 1 DIV, revealing only isolated cells present throughout the culture period. Previous studies of dissociated ganglion cells have found that TRPV4 activation through synthetic agonists induces apoptosis, which is consistent with our results [3].

The early downregulation of GS in CT and GSK explants may exacerbate the degeneration of ganglion cells. In the retina, Müller cell GS catalyses the conversion of excitatory amino acid glutamate to non-excitatory glutamine [22]. The loss of this protein is associated with an increase in extracellular glutamate, which, in addition to being continually released by

photoreceptors, has been found to be discharged by injured neurons, leading to excitotoxicity and an exacerbation of glial reactivity [22-24]. Ganglion cells are known to be particularly susceptible to excitotoxic insult [25,26]. In accordance, RN explants, which displayed an increased expression of of GS compared to the other explant groups, revealed that ganglion cells survived in greater numbers compared to all other groups. These results may be of particular interest in glaucoma research, where TRPV4 activation through increased intraocular pressure, as well as glutamate excitotoxicity and gliosis, is thought to contribute to ganglion cell death [26, 27].

4.2 Glial reactivity

Activation of TRPV4, and the resultant Ca2+ influx, has previously been reported to mediate Müller cell reactivity [3, 28]. However, Trpv4-/- mice display GFAP upregulation in Müller cells in the absence of experimental interventions, suggesting that a baseline TRPV4 activation is required for glial health [30]. In this experiment, GFAP labeling of explants treated with TRPV4 effectors (GSK and RN cultures) paradoxically revealed a low level of GFAP expression compared to CT explants after 5 DIV, suggesting an arrested gliotic response. However, other signs of glial reactivity were present in GSK cultures, which, in similarity to CT specimens, showed a downregulation of GS compared to in vivo controls and RN counterparts [22]. Also, despite the attenuation of GFAP upregulation, GSK specimens displayed similar patterns of neuronal cell death (NeuN), apoptosis (TUNEL) and overall morphology (HTX) at all time points when compared to CT counterparts. We have previously shown using the adult porcine explant model, that severe insults, such as treatment with the alkylating carcinogen N-methyl-N-nitrosourea (MNU), can result in neuronal cell death despite an apparent lack of the expected increase in GFAP [31].

A possible explanation for the lack of GFAP expression in the GSK explants may involve a direct interaction between the C-terminal domain of TRPV4 and cytoskeletal proteins, which has been reported for actin and β-tubulin, as well as the indirect influence on cytoskeletal polymerization through Ca2+ influx [29,30]. Further research is required to establish the mechanism behind this phenomenon.

4.3 TRPV4 signaling and neuronal degeneration

TRPV4 signaling is not tonic in nature, and can be sensitized to activation, an event seen during inflammatory conditions [32]. Also, the expression of TRPV4 can be downregulated by various forms of ligand binding, including GSK activation [17]. We found a rapid and sustained downregulation of TRPV4 expression in CT as well as in GSK treated explants, whereas the RN specimens maintained an expression pattern similar to that observed in the in vivo control, even after 5 DIV. During the dissection and culture procedure, it is possible that TRPV4 ligands such as cytochrome p450-derived metabolites and polyunsaturated fatty acids are released by damaged cells, causing detrimental TRPV4 activity [28]. This scenario may explain the degenerative damage seen in CT and GSK explants, whereas RN-1734 treatment putatively blocks the over-activation of TRPV4, leading to an enhanced neuronal survival and attenuated gliotic response, although the exact mechanism remains to be elucidated.

Although the maintenance of the retinal laminar architecture was improved in RN-treated cultures, apoptotic cell death was observed, mainly in the outer layers. The standard culture procedure employed in this work involves removing the retina from the normal pressurized environment of the eye and placing the explants with their pliable inner and outer segments against the culture membrane, causing the retina to become distorted - in similarity to the condition of retinal detachment [12]. We have previously shown that the addition of lateral stretch to the retinal sheet, or providing the explants with support to the inner retina, which

prevents this distortion, results in a significantly enhanced photoreceptor survival and a maintenance of inner and outer segments [13]. This implies that the tissue biomechanics have a significant influence on homeostasis. TRPV4 has previously been suggested to be one of the main mechanosensors of the retina, and that modulating the activity of this receptor may allow for greater tissue resilience to mechanical disturbance [3,5,12,13]. However, our results suggest that altering TRPV4 signaling alone cannot compensate for detrimental changes in the biomechanical environment. **Further research is needed to establish the exact mechanism through which the tissue response to biomechanical disruption is mediated and the possible role of TRPV4 in this setting.**

4.4 Summary

To summarize, we in this paper have explored the effects of modulating signaling through TRPV4 in an in vitro model of retinal degeneration. Specimens cultured with specific TRPV4 inhibitor RN-1734 displayed a significantly increased ganglion cell survival as well as a preservation of the retinal laminar architecture for up to 5 DIV, with an attenuation of the gliotic response and maintenance of glial homeostatic mediator GS. In contrast, control explants, as well as explants treated with specific TRPV4 agonist GSK1016790A, displayed extensive degenerative changes and retinal remodeling. The relationship presented herein between TRPV4 signaling and retinal cell health in vitro presents an interesting avenue of research into retinal degeneration, specifically with regard to glaucoma and retinal detachment.

5. FIGURE LEGENDS

Figure 1: Morphological staining and immunohistochemical labeling of normal adult porcine retina. A) Hematoxylin and eosin staining show well-populated cell layers with a clear laminar architecture. B) NeuN-labeling of ganglion cells display numerous large cell bodies present in a monolayer in the ganglion cell layer. C) Recoverin labeling of photoreceptors show labeled cell bodies in the outer nuclear layer as well as inner and outer segments. D) GFAP labeling is present in astrocytes and Müller cell endfeet at the inner border, as well as scattered, thin vertical Müller cell processes spanning the innermost layers. E) GS labeling of Müller cells is present throughout the retinal layers, with stronger labeling seen at the innermost border of the retina. F) TRPV4 labeling is observed in the plexiform layers as well as in large cell bodies of ganglion morphology in the ganglion cell layer. G) A double labeling of TRPV4 (red) and NeuN (green) show strong TRPV4 labeling in the inner plexiform layer as well as in a strong, punctate pattern in NeuN labeled cell bodies. H) No TUNEL labeled cells are present within the retinal layers. Scale bar: A-F, H: 50 µm; G: 25 µm. Abbreviations: NPig = normal adult pig; GCL = ganglion cell layer; IPL = inner plexiform layer; INL = inner nuclear layer; OPL = outer plexiform layer; ONL = outer nuclear layer; IS = inner segments; OS = outer segments; RPE = retinal pigment epithelium.

Figure 2: Hematoxylin and eosin staining (A-I) and recoverin labeling (photoreceptors, J-R) of retinal explants cultured for 1-5 days in vitro (DIV). From right to left in each panel: column 1, control explants; column 2 GSK-treated (GSK) explants; column 3, RN-1734 (RN) treated explants. From top to bottom: row 1, 1 DIV; row 2, 2 DIV; row 3, 5 DIV. A-B) 1 DIV CT and GSK explants display a dissolving laminar architecture with numerous pyknotic cells and vacuoles (arrows) in all cell layers. C) RN counterparts reveal pyknotic cells mainly in the outer nuclear layer, with isolated condensed

cells present in the inner nuclear layer. D-F) 2 DIV CT and GSK specimens show thinning, pyknosis and vacuolization (arrow) in all cell layers, whereas corresponding RN specimens show preserved lamination with pyknotic cells mainly in the outer retina. G-H) 5 DIV CT and GSK explants reveal overall thinning, remodeling as well as pyknosis and vacuolization (arrows) throughout the specimens. I) RN counterparts display a preserved laminar architecture with pyknotic cells present in the ONL. J-L) 1 DIV CT, GSK, and RN explants show slightly disorganized labeling of the outer nuclear layer. M-O) After 2 DIV, CT and GSK specimens reveal labeling of a thin, disorganized ONL, whereas corresponding RN specimens display labeling of a well-delimited ONL. P-R) 5 DIV CT and GSK explants labeling of a highly disorganized ONL, whereas RN counterparts display a strong labeling of photoreceptors located in the ONL. Scale bar: 50 μm.

Figure 3: NeuN labeling of ganglion cells in retinal explants cultured for 1-5 days in vitro (DIV). From right to left: column 1, control explants; column 2 GSK-treated (GSK) explants; column 3, RN-1734 (RN) treated explants. From top to bottom: row 1, 1 DIV; row 2, 2 DIV; row 3, 5 DIV. A-B) 1 DIV CT and GSK explants show only scattered NeuN labeled cells. C) In contrast RN counterparts reveal numerous labeled large cell bodies in the ganglion cell layer. D-F) 2 DIV CT and GSK specimens show only isolated labeled cells, whereas corresponding RN specimens display a multitude of NeuN-positive cells. G-H) 5 DIV CT and GSK explants reveal only a few, isolated NeuN-labeled cells. I) RN counterparts display a multitude of large cell bodies labeled in the ganglion cell layer. M-O) Statistical analysis reveals a significant preservation of ganglion cells in RN cultures at all time points, whereas CT and GSK counterparts display a dramatic and progressive cell loss beginning already at 1 DIV. Scale bar: 50 μm. ***=$p<0.001$. Error bars SEM.

Figure 4: GFAP labeling of astrocytes and activated Müller cells in retinal explants cultured for 1-5 days in vitro (DIV). From right to left: column 1, control explants; column 2 GSK-treated (GSK) explants; column 3, RN-1734 (RN) treated explants. From top to bottom: row 1, 1 DIV; row 2, 2 DIV; row 3, 5 DIV. A-C) 1 DIV CT, GSK and RN explants show labeling in astrocytes at the inner border as well as in isolated Müller cell fibers vertically spanning the inner retina. D-F) 2 DIV specimens display a similar labeling pattern to that observed in 1 DIV counterparts. G) 5 DIV CT explants reveal strong GFAP labeling present throughout the retina in thick, hypertrophied Müller cell fibers. H-I) Corresponding GSK and RN specimens display labeling similar to that seen in 1 and 2 DIV counterparts. Scale bar: 50 μm. J) Statistical analysis of GFAP labeling labeling intensity in explants cultured for 5 days in vitro. Control (CT) explants display a significantly higher labeling intensity compared to all other groups. No significant difference in labeling intensity was found between the explants treated with TRPV4 effectors. **=$p<0.01$, ***=$p<0.001$. Error bars SEM.

Figure 5: GS labeling of Müller cells in retinal explants cultured for 1-5 days in vitro (DIV). From right to left: column 1, control explants; column 2 GSK-treated (GSK) explants; column 3, RN-1734 (RN) treated explants. From top to bottom: row 1, 1 DIV; row 2, 2 DIV; row 3, 5 DIV. A-C) 1 DIV CT, GSK and RN explants show labeling at the inner border, with RN specimens also showing labeling of isolated Müller cell fibers and the outer limiting membrane in the outermost retina. D-E) 2 DIV CT and GSK specimens display a similar labeling pattern to that observed in 1 DIV counterparts. F) 2DIV RN explants, in contrast, display increased GS expression present throughout the specimen. G-H) 5 DIV CT and GSK explants reveal labeling similar to that seen in 1 and 2 DIV counterparts. I) Corresponding RN specimens display strong labeling similar to that seen at 2 DIV. Scale bar:

50 µm. J-L) Statistical analysis of GS labeling labeling intensity in explants cultured for 1, 2 and 5 days in vitro. At 1 DIV, CT explants display significantly lower levels of GS expression compared to GSK and RN explants. After 2 DIV, RN specimens display a significantly higher labeling intensity compared to explants treated with GSK. After 5 DIV, this expression is maintained in RN retinas, and found to be significantly higher compared to corresponding CT and GSK specimens. **=$p<0.01$, ***=$p<0.001$. Error bars SEM.

Figure 6: TRPV4 labeling in retinal explants cultured for 1-5 days in vitro (DIV). From right to left: column 1, control explants; column 2 GSK-treated (GSK) explants; column 3, RN-1734 (RN) treated explants. From top to bottom: row 1, 1 DIV; row 2, 2 DIV; row 3, 5 DIV. A-B) 1 DIV CT and GSK explants show scattered labeling in the outer plexiform layer. C) RN counterparts reveal strong labeling in both plexiform layers as well as in large bodies of ganglion morphology, similar to that found in the normal adult control. D-E) 2 DIV CT and GSK specimens display a similar labeling pattern to that observed in 1 DIV counterparts. F) 2DIV RN explants, in contrast, display a maintained TRPV4 expression in the plexiform layers and ganglion cells. G-H) 5 DIV CT and GSK explants reveal very little TRPV4 labeling, similar to that seen in 1 and 2 DIV counterparts. I) Corresponding RN specimens display strong labeling of ganglion cells, with slightly weaker labeling present in the plexiform layers. Scale bar: 50 µm. J-L) Statistical analysis of TRPV4 labeling labeling intensity in explants cultured for 1, 2 and 5 days in vitro. RN explants show significant preservation of TRPV4 expression at all time points compared to CT and GSK counterparts. ***=$p<0.001$. Error bars SEM.

Figure 7: TUNEL labeling of apoptotic cells in retinal explants cultured for 1-5 days in vitro (DIV). From right to left: column 1, control explants; column 2 GSK-treated (GSK) explants; column 3, RN-1734 (RN) treated explants. From top to bottom: row 1, 1

DIV; row 2, 2 DIV; row 3, 5 DIV. A-B) 1 DIV CT and GSK explants show scattered labeled cells in all cell layers. C) RN counterparts reveal only weak labeling of scattered cells in the outermost retina. D-E) 2 DIV CT and GSK specimens display a similar labeling pattern to that observed in 1 DIV counterparts. F) 2 DIV RN explants, in contrast, show labeling of scattered cells in the inner and outer nuclear layer. G-I) 5 DIV CT, GSK, and RN explants reveal strong labeling of a multitude of cells throughout the specimen. Scale bar: 50 μm. J-L) Statistical analysis of TUNEL labeling labeling intensity in explants cultured for 1, 2 and 5 days in vitro. After 1 DIV, RN specimens display a significantly lower labeling intensity compared to CT counterparts. After 2 DIV, no significant difference in labeling intensity is found. After 5 DIV, CT explants display a significantly higher level of labeling compared to GSK and RN counterparts. *=$p<0.05$, **=$p<0.01$, ***=$p<0.001$. Error bars SEM.

Figure 8: Fluorescence intensity measurement of TUNEL labeling of the cell layers retinal explants cultured for 1-5 days in vitro (DIV). From right to left: column 1, 1 DIV explants; column 2, 2 DIV explants; column 3, 5 DIV explants. From top to bottom: row 1, ganglion cell layer (GCL); row 2, inner nuclear layer (INL); row 3, outer nuclear layer (ONL). Abbreviations: control explants =CT; GSK-treated explants = GSK; RN-1734-treated explants = RN. *=$p<0.05$, **=$p<0.01$, ***=$p<0.001$. Error bars SEM.

Supplemental figure 1: Figure 1G with the channels separated, showing TRPV4 labeling of ganglion cells and the inner plexiform layer (A), and NeuN labeling of ganglion cells (B). Scale bar 25 μm.

6. TABLES

Antigen	**Antibody name**	**Target cell/structure /protein**	**Species**	**Dilution**	**Source**
NeuN (Neuronal Nuclei)	Anti-Neuronal Nuclei	Ganglion cells	Mouse monoclonal	1:100	Millipore, Billerica, MA, USA
Recoverin	Anti-recoverin	Rod and cone photoreceptors	Rabbit polyclonal	1:10000	Chemicon International, CA, USA
GFAP	Anti-Glial Fibrillary Acidic Protein	Activated Müller cells, astrocytes	Mouse monoclonal	1:200	Chemicon International, CA, USA
Glutamine Synthetase	Anti-glutamine synthetase	Müller cells	Rabbit polyclonal	1:2000	Abcam, Cambridge, UK
TRPV4	Anti-TRPV4	Müller cells, ganglion cells	Rabbit polyclonal	1:300	Abcam, Cambridge, UK
2ndary Antibody	**Antibody name**	**Target**	**Species**	**Dilution**	**Source**
FITC	Anti-mouse IgG FITC conjugate	Anti-mouse	Goat	1:200	Sigma Aldrich, St Louis, MO, USA
FITC	Anti-rabbit IgG FITC conjugate	Anti-rabbit	Donkey	1:200	Abcam, Cambridge, UK
Rhodamine red	Rhodamine Red TM -X-conjugated	Anti-rabbit	Donkey	1:200	Jackson ImmunoResearch, PA, USA

Table 1. Table over primary and secondary antibodies used for immunohistochemical analysis.

7. ACKNOWLEDGEMENTS

The authors would like to thank Oscar Manouchehrian and Patricia Veiga-Crespo for technical assistance, as well as Peter Zygmunt and C. Ross Ethier for excellent ideas and stimulating discussion.

8. DECLARATION OF INTEREST

The authors declare no competing financial interest.

9. FUNDING

This work has been supported by: The Faculty of Medicine at Lund University, The Swedish Research Council (2015-02772), The Trust for Visually Impaired in Malmöhus County, Carmen and Bertil Regnérs Trust, Maggie Stephens Trust, The King Gustaf V and Queen Victoria Freemason Foundation, Karin Sandqvist Trust.

10. REFERENCES

1. Everaerts W, Nilius B, Owsianik G. The vanilloid transient receptor potential channel TRPV4: from structure to disease. Prog Biophys Mol Biol. 2010;103(1):2-17.

2. Lee JC, Choe SY. Age-related changes in the distribution of transient receptor potential vanilloid 4 channel (TRPV4) in the central nervous system of rats. J Mol Histol. 2014;45(5):497-505.

3. Ryskamp DA et al. The polymodal ion channel transient receptor potential vanilloid 4 modulates calcium flux, spiking rate, and apoptosis of mouse retinal ganglion cells. J Neurosci. 2011;31(19):7089-101.

4. Butenko OJ et al. The increased activity of TRPV4 channel in the astrocytes of the adult rat hippocampus after cerebral hypoxia/ischemia. PLoS One. 2012;7(6):e39959.

5. Matthews BD et al. Ultra-rapid activation of TRPV4 ion channels by mechanical forces applied to cell surface β1 integrins. Integrative biology : quantitative biosciences from nano to macro. 2010;2(9):435-442.

6. Jang Y et al. Axonal neuropathy-associated TRPV4 regulates neurotrophic factor-derived axonal growth. J Biol Chem. 2012;287(8):6014-24.

7. Shi M et al. Glial cell-expressed mechanosensitive channel TRPV4 mediates infrasound-induced neuronal impairment. Acta Neuropathol. 2013;126(5):725-39.

8. Ryskamp DA et al. Swelling and eicosanoid metabolites differentially gate TRPV4 channels in retinal neurons and glia. J Neurosci. 2014;34(47):15689-700.

9. Winkler J et al. Cellular and cytoskeletal dynamics within organ cultures of porcine neuroretina. Exp Eye Res. 2002;74(6):777-88.

10. Kobuch K et al. Maintenance of adult porcine retina and retinal pigment epithelium in perfusion culture: characterisation of an organotypic in vitro model. Exp Eye Res. 2008;86(4):661-8

11. Fernandez-Bueno I et al. Müller and macrophage-like cell interactions in an organotypic culture of porcine neuroretina. Mol Vis. 2008;14:2148-56.

12. Taylor L et al. Feet on the ground: Physical support of the inner retina is a strong determinant for cell survival and structural preservation in vitro. Invest Ophthalmol Vis Sci. 2014;55(4):2200-13.

13. Taylor L et al. Stretch to see: lateral tension strongly determines cell survival in long-term cultures of adult porcine retina. Invest Ophthalmol Vis Sci. 2013;54(3):1845-56.

14. Ghosh F et al. In vitro biomechanical modulation-retinal detachment in a box. Graefes Arch Clin Exp Ophthalmol. 2016;254(3):475-87.

15. Taylor L et al. Effects of glial cell line-derived neurotrophic factor on the cultured adult full-thickness porcine retina. Curr Eye Res. 2013;38(4):503-15.

16. Kaempf S et al. Novel organotypic culture model of adult mammalian neurosensory retina in co-culture with retinal pigment epithelium. J Neurosci Methods. 2008;173(1):47-58.

17. Jin M et al. Determinants of TRPV4 activity following selective activation by small molecule agonist GSK1016790A. PLoS One. 2011;6(2):e16713.

18. Vincent F et al. Identification and characterization of novel TRPV4 modulators. Biochem Biophys Res Commun. 2009;389(3):490-4.

19. Albert ES et al. TRPV4 channels mediate the infrared laser-evoked response in sensory neurons. J Neurophysiol 2012;107(12):3227-34.

20. Manouchehrian O et al. Who let the dogs out?: detrimental role of Galectin-3 in hypoperfusion-induced retinal degeneration. J Neuroinflammation. 2015;12(1):92.

21. Shen S et al. Retinal ganglion cells lose trophic responsiveness after axotomy. Neuron. 1999;23:285–295.

22. Bringmann A et al. Müller cells in the healthy and diseased retina. Prog Retin Eye Res. 2006;25(4):397-424.

23. Lewis GP et al. Changes in the expression of specific Müller cell proteins during long-term retinal detachment. Exp Eye Res. 1989;49(1):93-111.

24. Lewis GP et al. Rapid changes in the expression of glial cell proteins caused by experimental retinal detachment. Am J Ophthalmol. 1994;118(3):368-76.

25. Luo X et al. Selective excitotoxic degeneration of adult pig retinal ganglion cells in vitro. Invest Ophthalmol Vis Sci. 2001;42(5):1096-106.

26. Kuehn MH et al. Retinal ganglion cell death in glaucoma: mechanisms and neuroprotective strategies. Ophthalmol Clin North Am. 2005;18(3):383-95

27. Križaj D et al. From mechanosensitivity to inflammatory responses: new players in the pathology of glaucoma. Curr Eye Res. 2014;39(2):105-19.

28. Ryskamp DA et al. TRPV4 links inflammatory signaling and neuroglial swelling. Channels (Austin). 2015;9(2):70-2.

29. Zaninetti R et al. Activation of TRPV4 channels reduces migration of immortalized neuroendocrine cells. J Neurochem. 2011;116(4):606-15.

30. Takahashi N et al. TRPV4 channel activity is modulated by direct interaction of the ankyrin domain to PI(4,5)P_2. Nat Commun. 2014;5:4994.

31. Taylor L et al. N-methyl-N-nitrosourea-induced neuronal cell death in a large animal model of retinal degeneration in vitro. Exp Eye Res. 2016;26;148:55-64.

32. Vriens J et al. Pharmacology of vanilloid transient receptor potential cation channels. Mol Pharmacol. 2009;75(6):1262-79.

33. Vincent F et al. Identification and characterization of novel TRPV4 modulators. Biochem Biophys Res Commun. 2009 Nov 20;389(3):490-4.

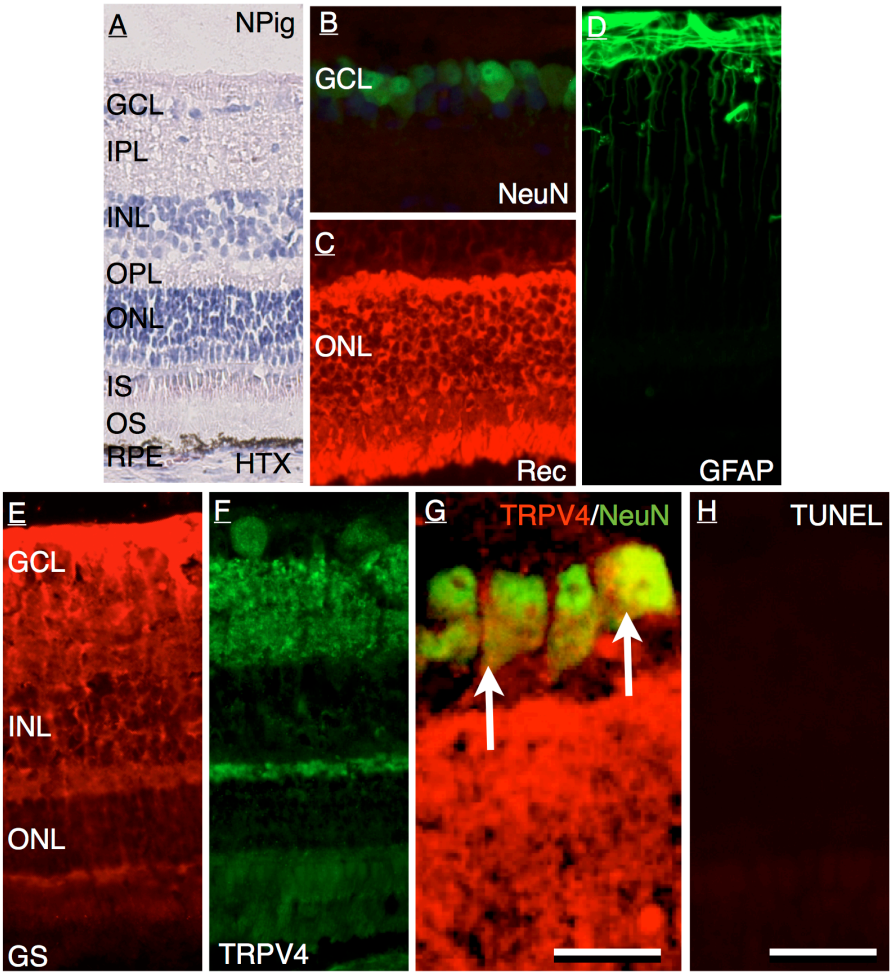

Figure 1, Taylor et al.

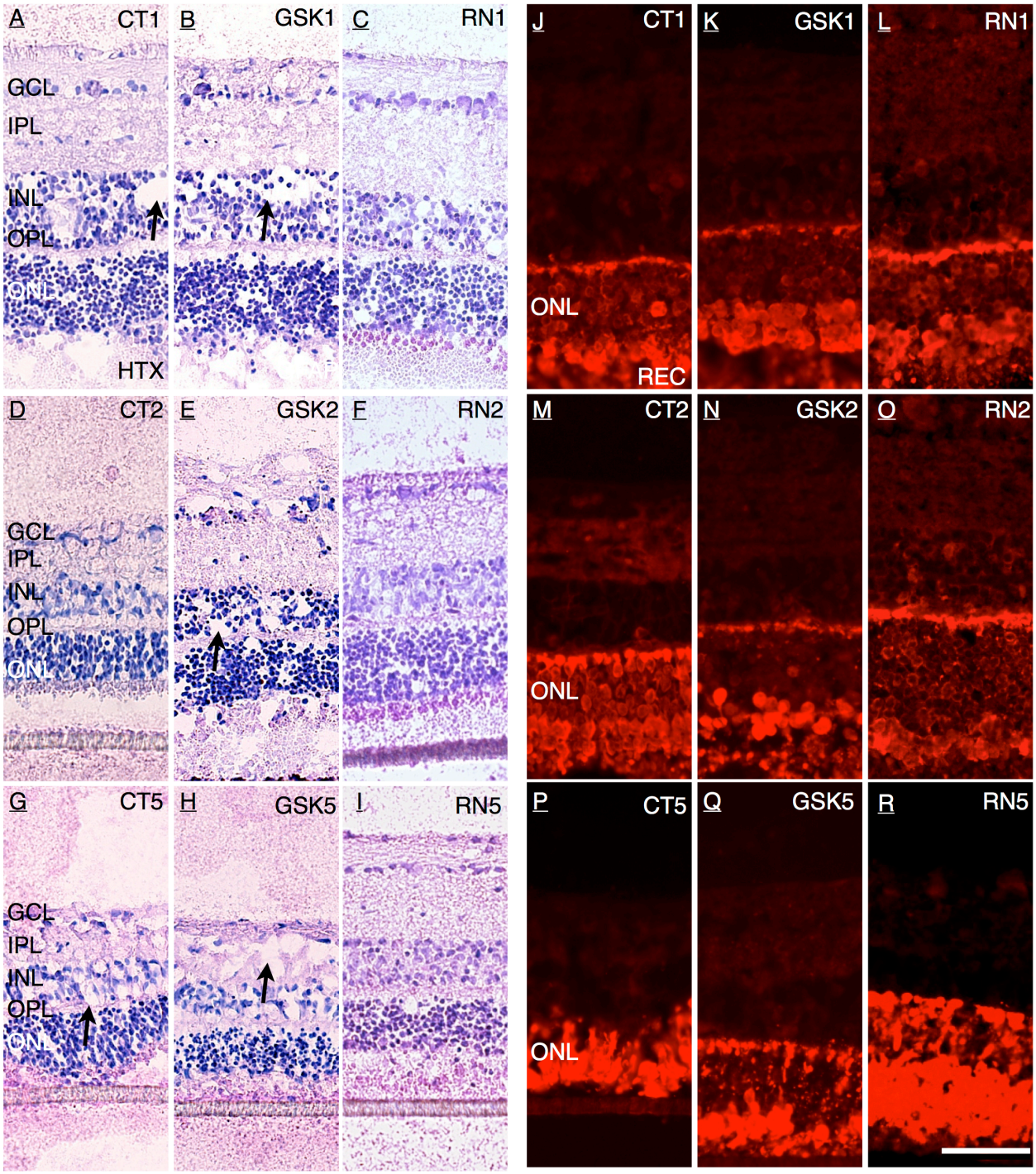

Figure 2, Taylor et al.

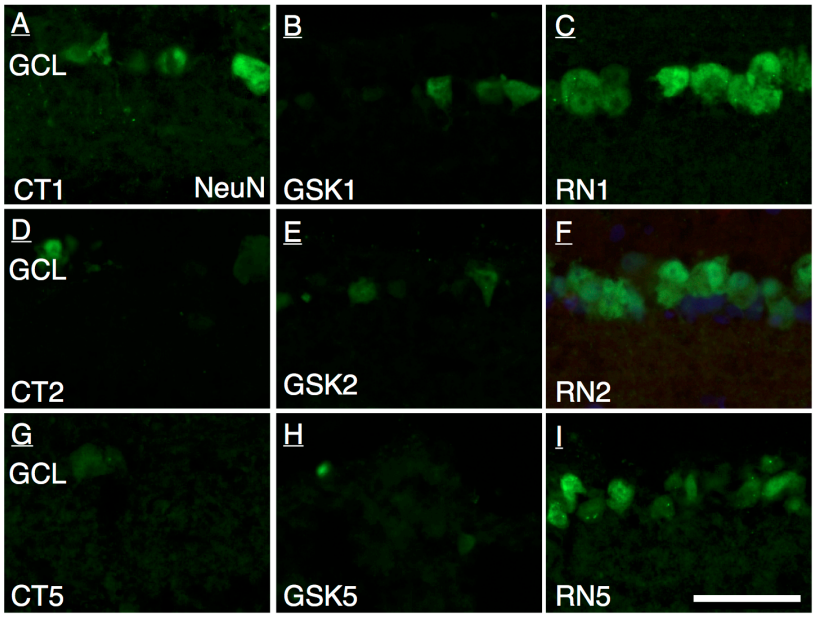

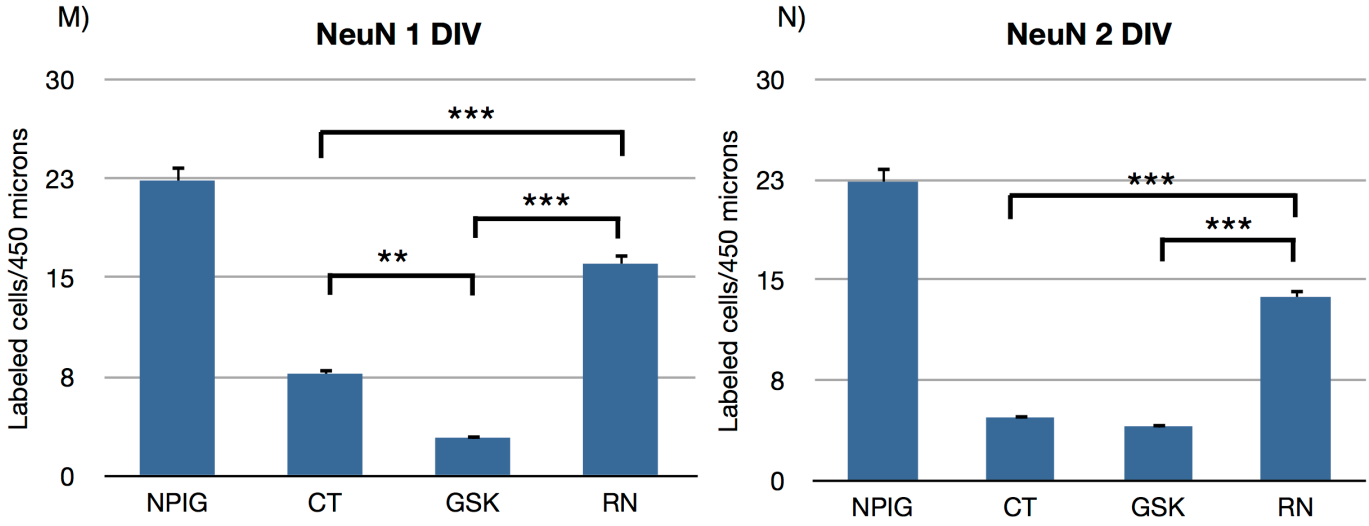

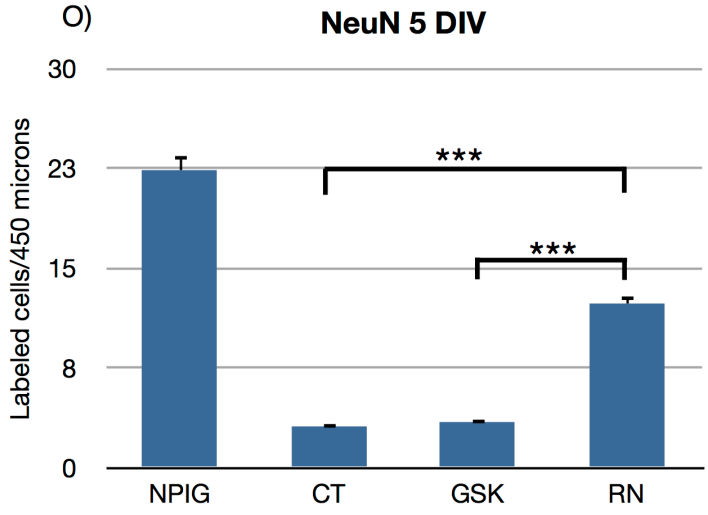

Figure 3, Taylor et al.

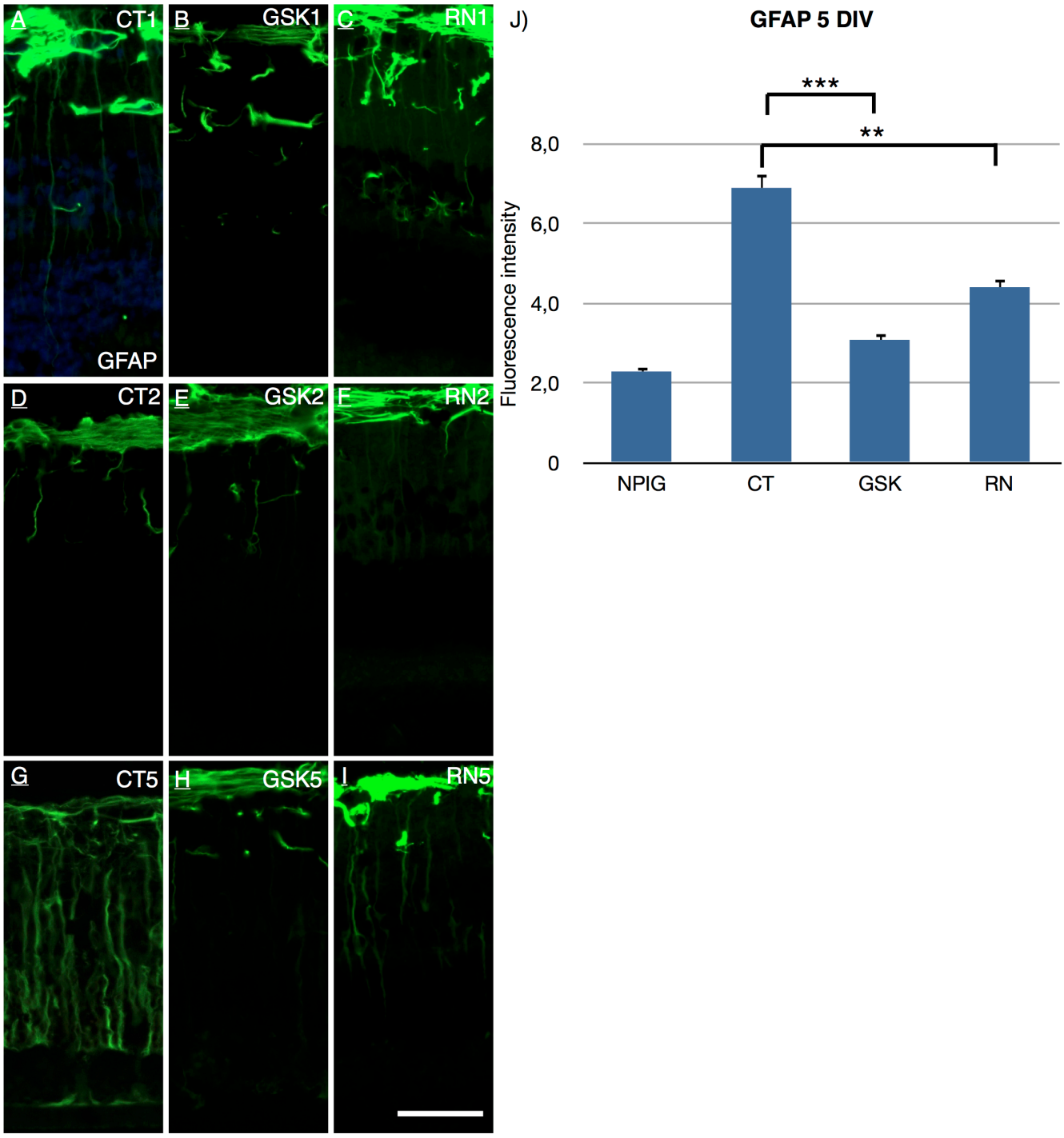

Figure 4, Taylor et al.

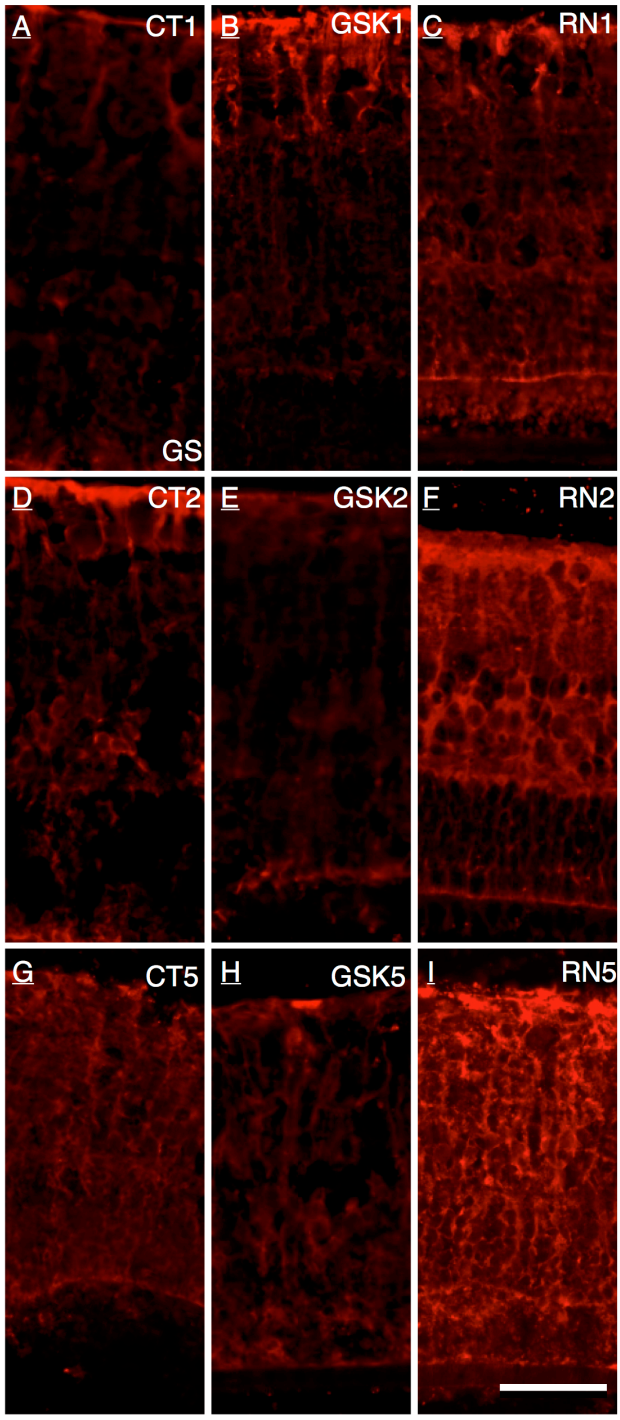

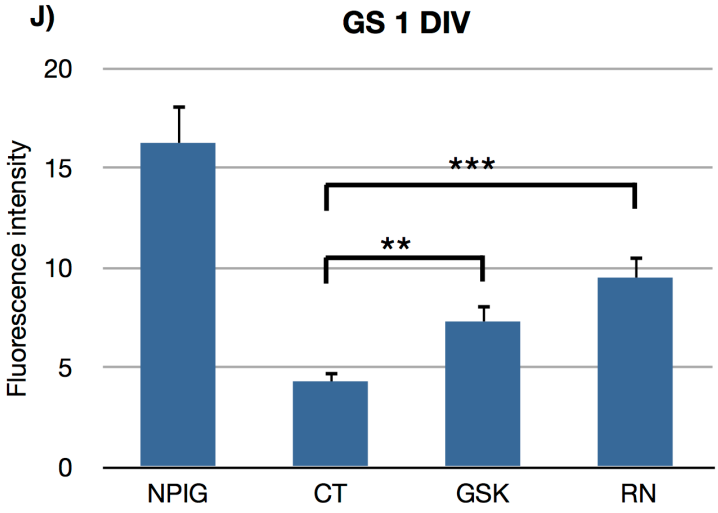

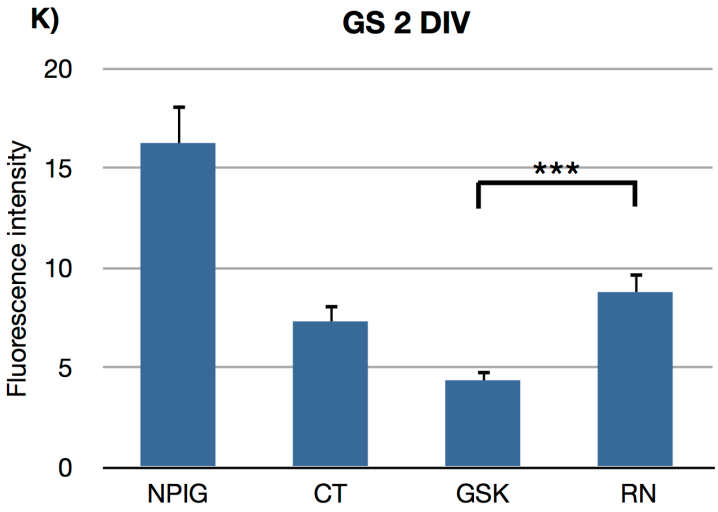

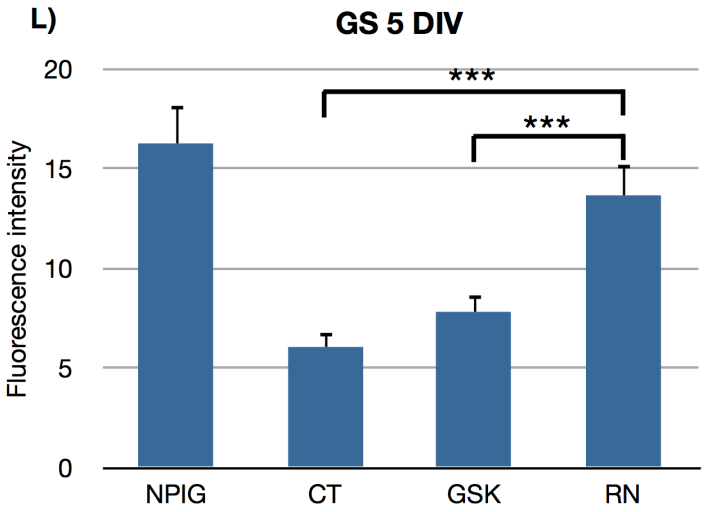

Figure 5, Taylor et al.

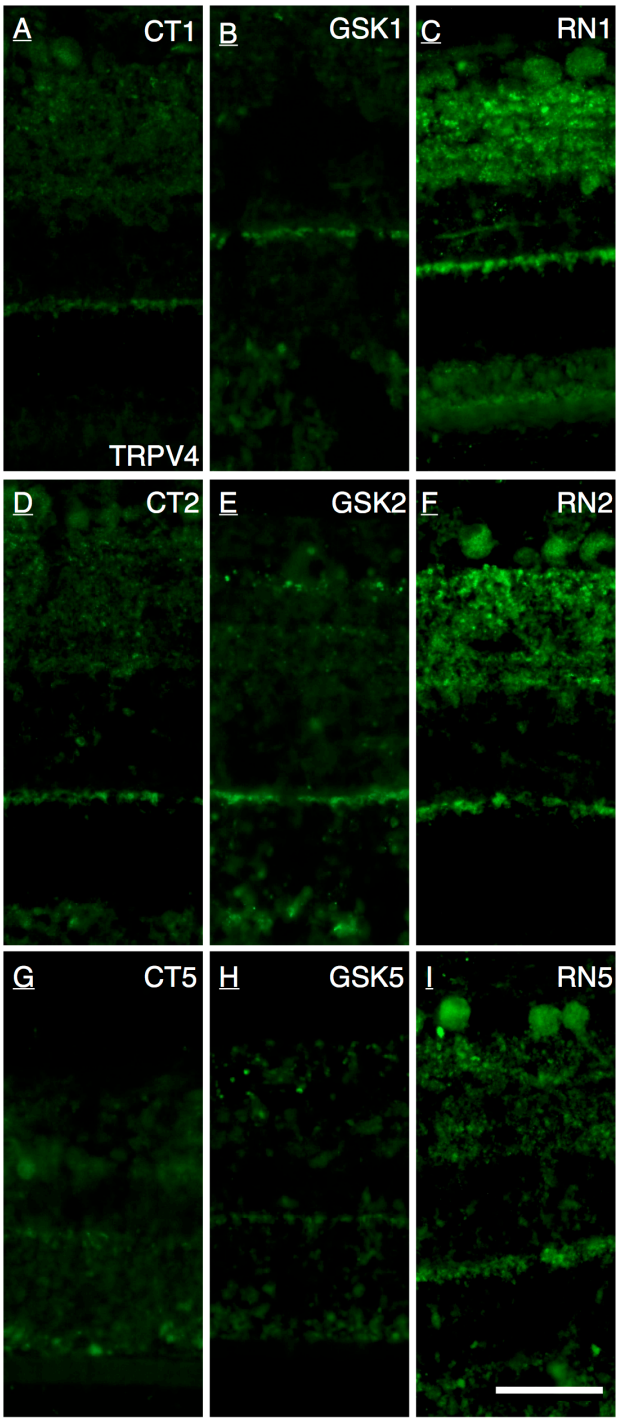

Figure 6, Taylor et al.

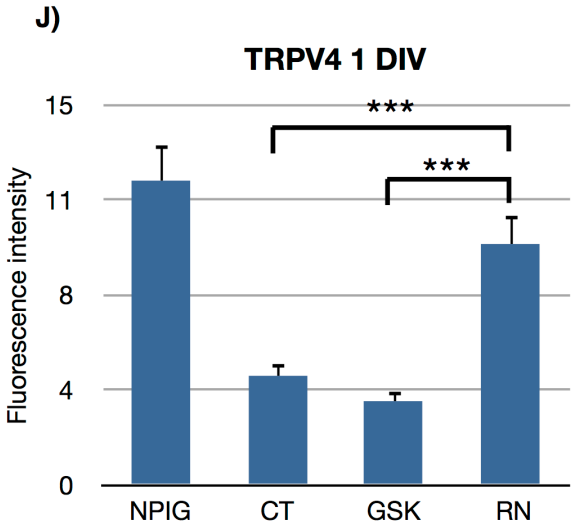

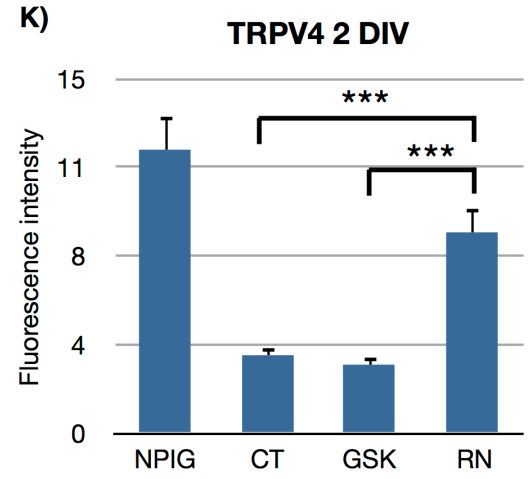

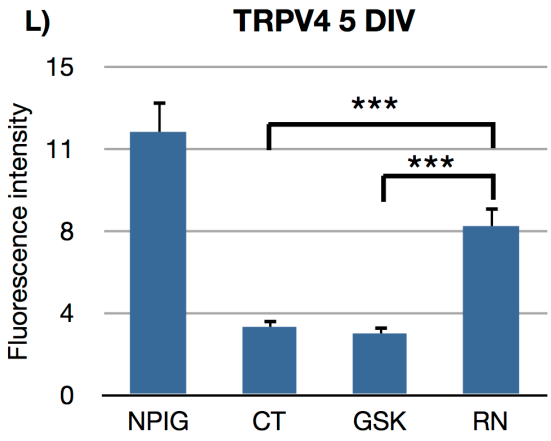

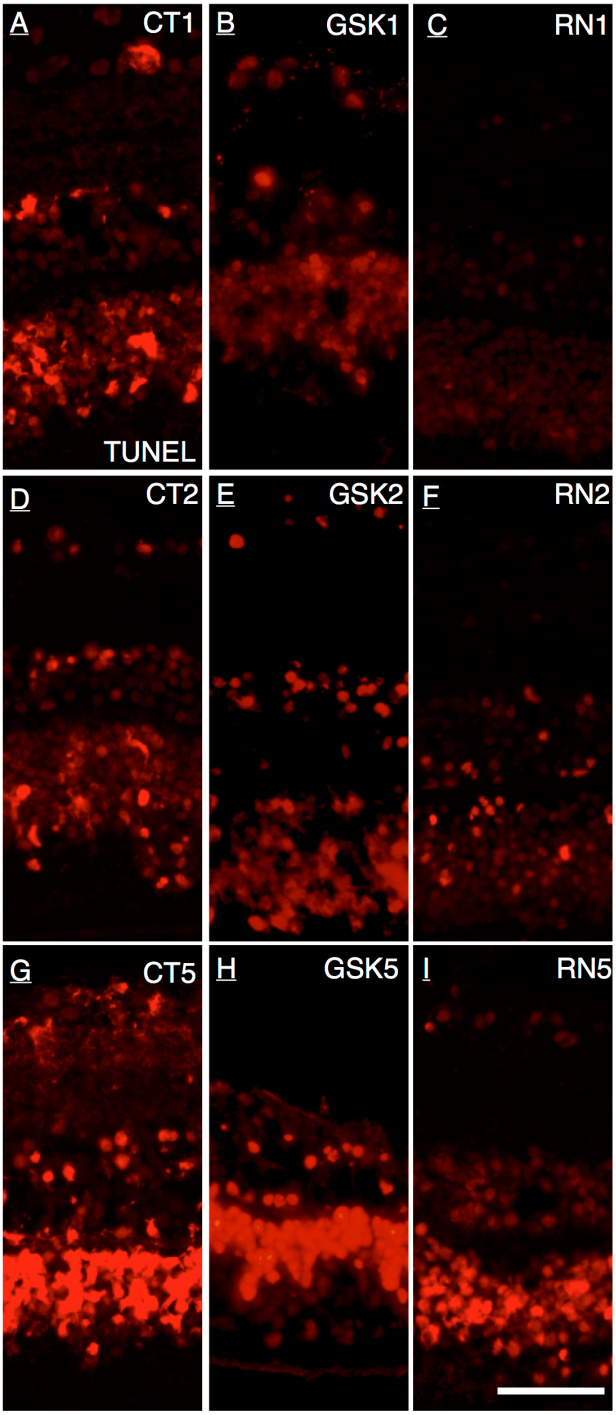

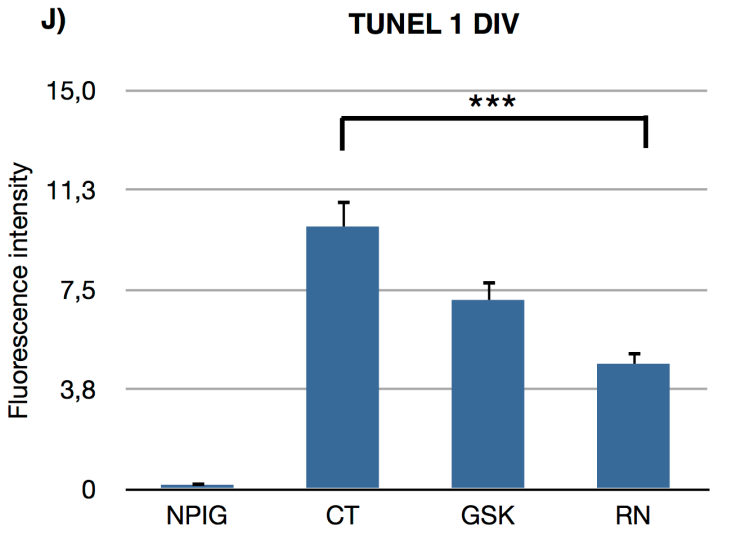

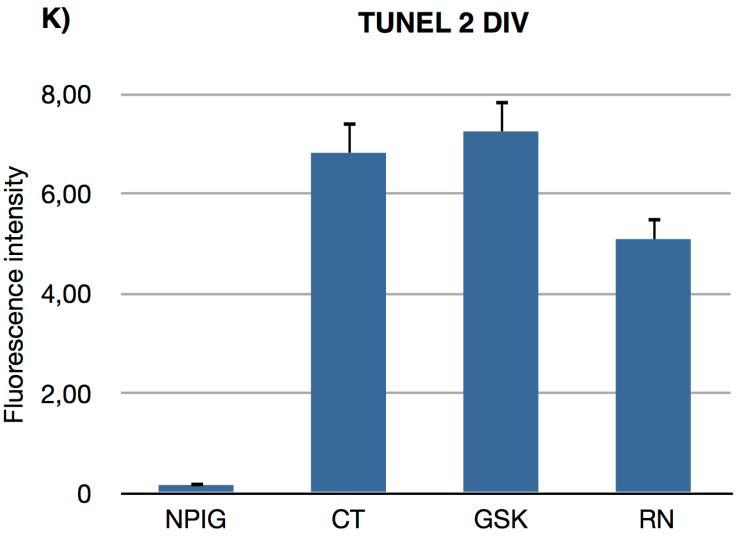

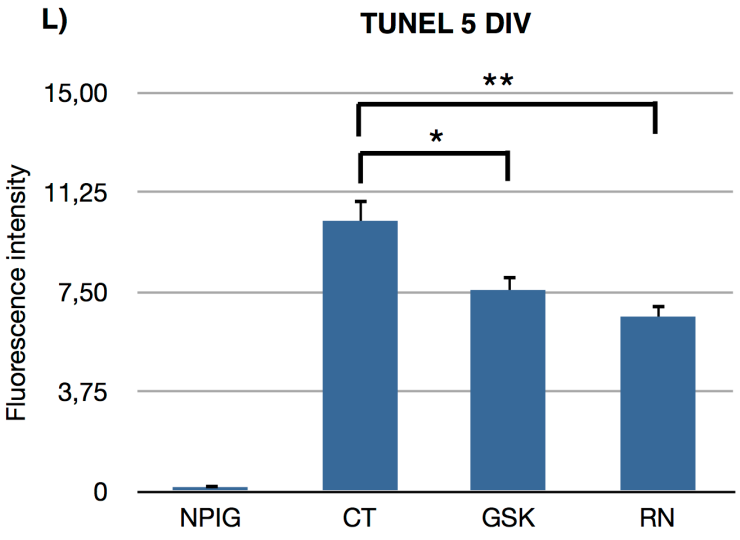

Figure 7, Taylor et al.

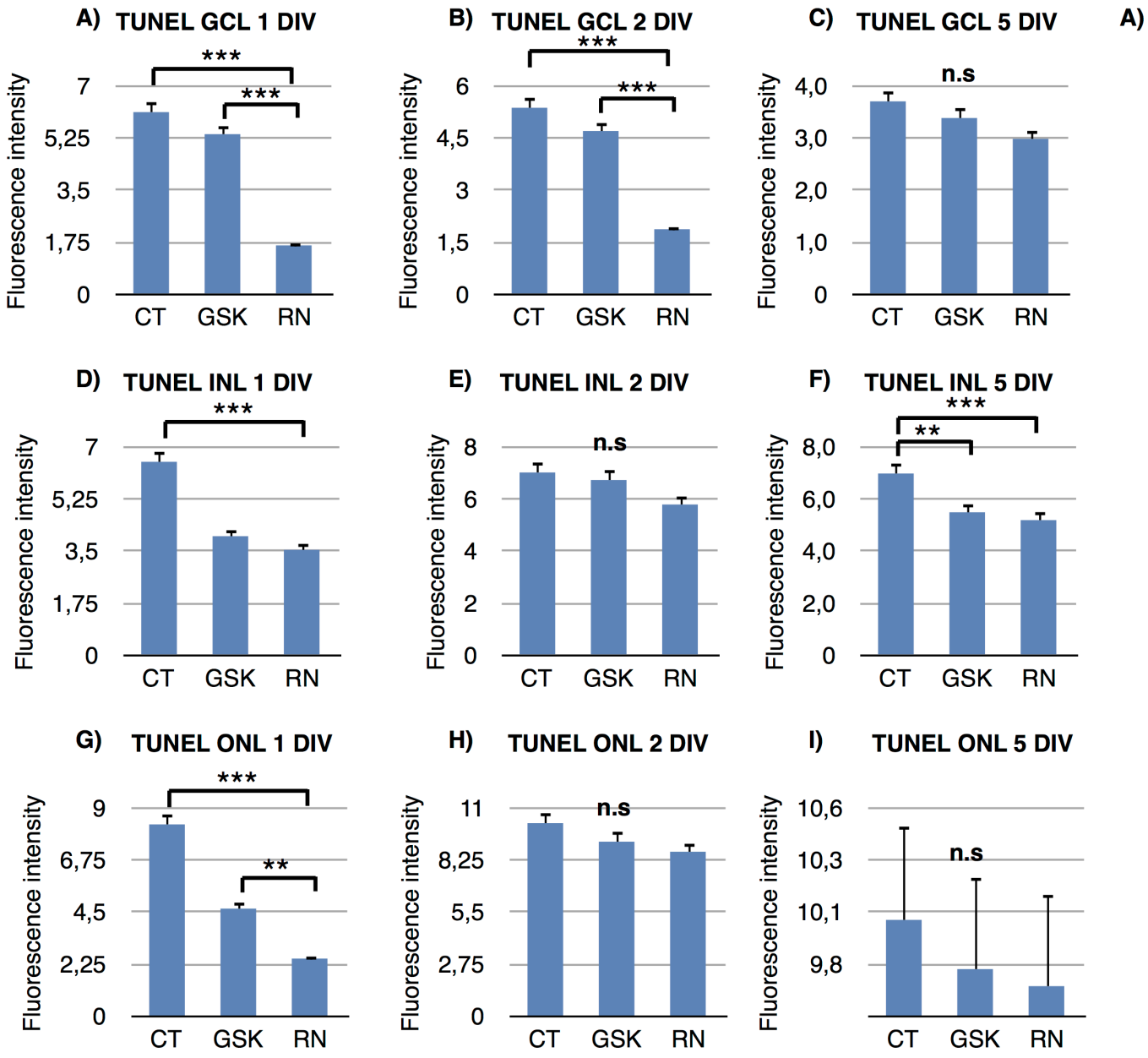

Figure 8, Taylor et al.